Chapter

Improvement of the Thermal Properties of Sorel Cements

Rim Zgueb, Amal Brichni and Noureddine Yacoubi

Abstract

Sorel cements is a promising building material for insulation applications. Indeed, the effect of polyvinyl acetate polymer on cements has been investigated. The polyvinyl acetate polymer was added to the cement matrix with a percentage of 0, 5, 10, 15 and 20% by weight of Sorel cement. The thermal properties of Sorel cement were determined by photothermal deflection technique. Thermal properties such as thermal conductivity and thermal diffusivity are measured by coincidentally the experimental curves of the photothermal signal with the best corresponding theoretical curves. The results revealed that the incorporation of polyvinyl acetate polymer enhance the thermal insulation and reduce the compressive strength of Sorel cement.

Keywords: Sorel cement, photothermal deflection technique, thermal insulation, mechanical properties, polyvinyl acetate polymer

1. Introduction

Thermal insulation consists in using a material or a combination of materials in order to limit heat losses by conduction, convection and radiation between the interior and exterior of a building due to its low thermal conductivity. Thus, thermal insulation acts as a thermal barrier. The two main criteria for thermal insulation of buildings are the optimization of energy consumption and the protection of buildings against climatic factors. In some countries, people spend up to 90% of their time indoors (offices, factory, workshops, homes, ...) so they need a viable artificial environment that requires energy. Thermal insulation reduces heat loss, saves heating, limits greenhouse gas emissions, and improves living comfort.

In addition, cement will remain the main material that meets the needs of modern infrastructure and participates in the construction of large structures. Thus the development of cement performance to meet current needs has prompted several research projects to improve its thermal insulation without reducing its resistance.

One of the most promising cements for thermal insulation is magnesium oxychloride cement (MOC). During the last decade, the development of magnesium oxychloride cement was motivated by environmental considerations. The MgO production temperature was lower than the conversion temperature of $CaCO_3$ into Portland cement. The energy savings associated with this reduced temperature have led many researchers to believe that magnesium oxychloride cements are the future of green cement. In addition, MgO has the capacity to potentially absorb CO_2

unlike Portland cement. It is "carbon neuter" cement. These two interdependent aspects have a recent academic and commercial interest in the field of MgO cements.

MOC cement is synthesized by dissolving the magnesia MgO into aqueous solution of magnesium chloride hexahydrate $MgCl_2$, forming a homogeneous gel from which the basic salts of magnesium chloride precipitate. These salts are expressed by $xMg(OH)_2.yMgCl_2.zH_2O$ phases which depend on the temperature, the reactivity of magnesium and the relationships between the number of moles of $MgCl_2$ to that of the water molecules, the temperature and the reactivity of magnesium [1]. It has several performances and has become popular due to its attractive appearance, similar to that of marble. Indeed, it rapid hardening rate and it has high mechanical strength and good resistance to abrasion. The abrasion resistance is three times that of ordinary Portland cement. Generally, the compressive strength is greater than 50 MPa after curing for 28 days [2–7]. In addition, a peculiarity of this cement is its resistance to salt and saline solutions. The main applications used are architectural applications such as the construction of thermal and acoustical insulating panels [8], the construction of industrial floors and other prefabricated building boards [9].

In this chapter, we investigated the thermal properties of Sorel cement. The aim of this research was to improve the thermal insulation of Sorel cement by using a polyvinyl acetate (PVAc) polymer. We have determined the thermal conductivity and thermal diffusivity of various blended PVAc cements and we are studying the effect of PVAc on the compressive strength of composite materials.

2. Experimental procedures

2.1 Specimen preparation

The main materials used to synthesize the MOC are Magnesia (MgO), magnesium chloride ($MgCl_2$) and water (H_2O). Magnesium oxide powder used in this study is mostly produced by calcinations of magnesite powder (HiMedia, India) at a temperature around 900°C. We dissolved magnesium chloride hexahydrate (Scharlab, Spain) in distilled water to prepare a saturated solution of magnesium chloride. The mass concentration of the solution was 217 g for 100 g of water. The mass ratio of $MgCl_2.6H_2O/MgO = 2.22$ [10]. The PVAc polymer (SICOP, Tunisia) is a fluid of low cost whose viscosity at 20°C is 10,000 ± 500 Pa s and the PH = 6 ± 1.

The samples were prepared by mixing at the same time magnesium oxide powder, saturated magnesium chloride solution and PVAc polymer. The polyvinyl acetate polymer is replaced by MgO. Five samples are synthesized; four samples with the incorporation of PVAc and a control sample (without addition). The obtained samples which are SC0 (0% PVAC), SC5 (5% PVAC), SC10 (10% PVAC), SC15 (15% PVAC) and SC20 (20% PVAC). The mixtures were cast into the cylindrical molds of height 50 mm and diameter about 25 mm, stored for 24 h, then unmolded and air-cured for 28 days.

2.2 Methods

The compressive strength of specimens was tested using Liyold mechanical testing instrument with a load of 300 KN. At the age of 28 days, the compressive strength for samples with diameter 25 mm and height 50 mm were measured at a loading speed of 2 mm/min at ambient temperature.

Measurement of thermal conductivity was performed in dry state using the photothermal deflection technique.

The micro-morphology on the fractured surface of MOC was characterized by scanning electron microscopy (SEM, JEOL-JSM- 5400). The sample is previously coated with a layer of gold and SEM was operated at 15 kV of acceleration voltage.

3. Photothermal deflection technique

3.1 Principle of the photothermal deflection technique PTD

The sample is heated by modulated and uniform light pump beam. The optical absorption of the sample will generate a unidimentional thermal wave that will propagate into the sample and in the surrounding fluid near the surface of the sample, inducing a temperature gradient then a refractive index gradient in the fluid. The absorbed light is transformed into heat by a nonradiative de-excitation process. A laser beam skimming parallely the sample surface and passing through this refractive index gradient is deflected. This deflection is related to the thermal and optical properties of the sample.

The deflection of the probe laser beam ψ is complex number $\left(\psi = |\psi| e^{j\varphi}\right)$ given by [11]:

$$\psi(z,\ t) = \frac{L}{n_0}\frac{dn}{dT_f}\frac{\sqrt{2}}{\mu_f} \quad |T_0| \quad e^{-\frac{z_0}{\mu_f}}\ e^{j\left(\theta+\frac{\pi}{4}-\frac{z_0}{\mu_f}\right)}\ e^{j\omega t} \tag{1}$$

T_0 which is the periodic temperature rise at the sample surface is a complex number that written $T_0 = |T_0| e^{j\theta}$, Z_0 is the distance between the probe laser beam axis and the sample surface, L is the sample length in the direction of the laser probe beam, n is the fluid refractive index. Where $(\mu_f = D_f/\pi f)^{1/2}$ is the thermal diffusion length of the fluid with D_f the thermal diffusivity of the fluid and $j^2 = -1$.| ψ| and φ are respectively the amplitude and the argument of the laser pump beam deflection given by:

$$|\psi(z)| = -\frac{L}{n_0}\frac{dn}{dT_f}\frac{\sqrt{2}}{\mu_f}\ |T_0|\ e^{-\frac{z_0}{\mu_f}} \tag{2}$$

$$\varphi = \frac{-z_0}{\mu_f} + \theta + \frac{\pi}{4} \tag{3}$$

In order to determine the deflection of the probe laser beam, we have to calculate the periodic temperature T_0 at the sample surface.

3.2 Calculation of the periodic elevation temperature T_0 at the sample surface

3.2.1 Bulk sample

3.2.1.1 Calculation of T_0

The sample consists of only one layer (**Figure 1**) of thermal conductivity k_s, thermal diffusivity D_s and thickness l_s. It is fixed at backing of k_b, D_b, l_b respectively thermal conductivity, thermal diffusivity and thickness. The sample and backing are in a fluid (air) of thermal conductivity k_f, thermal diffusivity D_f and thickness l_f. T_o determine

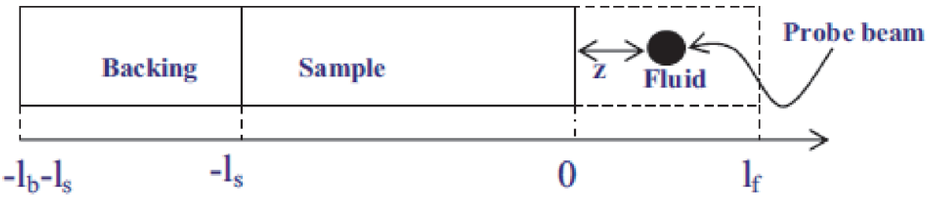

Figure 1.
Different medium browsed by the heat.

the periodic temperature T_0, we solve the one-dimensional heat diffusion equation in the different media backing, sample and fluid. Assuming that only the sample is absorbing the pump light beam, the heat equations in the different media are given by:

$$\begin{aligned} \frac{\partial^2 T_f}{\partial z^2} &= \frac{1}{D_f}\frac{\partial T_f}{\partial t} && \text{if } 0 \le z \le l_f \\ \frac{\partial^2 T_s}{\partial z^2} &= \frac{1}{D_s}\frac{\partial T_s}{\partial t} - Ae^{\alpha z}\left(1 + e^{j\omega t}\right) && \text{if } -l_s \le z \le 0 \\ \frac{\partial^2 T_b}{\partial z^2} &= \frac{1}{D_b}\frac{\partial T_b}{\partial t} && \text{if } -l_s - l_b \le z \le -l_s \end{aligned} \tag{4}$$

where $A = \alpha_s I_0/2ks$ are constant numbers and α_s is the optical absorption coefficient of the sample.

Indeed, the application of the boundary conditions of temperature and heat flux at the different interfaces allows us to determine the expression of the periodic temperature T_0 at the sample surface:

$$\begin{aligned} T_0 = -E\,\big[&(1-r)(1+b)\,e^{\sigma_s l_s} - (1+r)(1-b)\,e^{-\sigma_s l_s} \\ &+ 2(r-b)\,e^{-\alpha l_s}\big] / \big[(1+g)\,(1+b)\;e^{\sigma_s l_s} - (1-g)(1-b)\;e^{-\sigma_s l_s}\big] \end{aligned} \tag{5}$$

3.2.1.2 Illustration of theoretical model

We will study in this paragraph the variations of the photothermal signal as a function of the square root of the frequency in the case of a bulk sample. **Figure 2** represents the theoretical variations normalized amplitude and phase of the photothermal signal as a function of the square root of the frequency for three values of the thermal conductivity (k = 0.1, 2.0 and 4.0 W/m K) of a bulk sample.

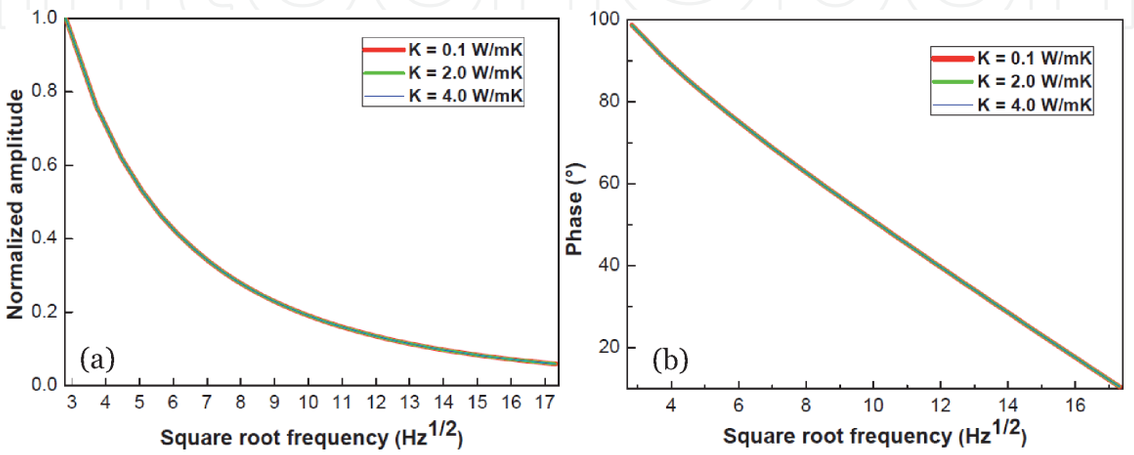

Figure 2.
Theoretical variation of the normalized amplitude (a) and phase (b) of the photothermal signal with the square root of modulation frequency for three numerical values of thermal conductivity.

We see that the normalized amplitude and the phase of the PTD signal are insensitive to variations of k (the three curves are coincident), which means that in this case we cannot determine the thermal conductivity of the sample.

Figure 3 represents the theoretical variations normalized amplitude and phase curves for different values of thermal diffusivity D. These curves show a remarkable sensitivity of the PTD signal to variations in thermal diffusivity, which allows determining thermal diffusivity with great precision.

3.2.2 Sample composed (layer deposed on a substrate)

3.2.2.1 Calculation of T_0

The sample is composed of a layer deposed on a substrate (**Figure 4**). Fernelius [10] was developed the theoretical model of a layer deposed on a substrate by writing the heat equations in the four medium: fluid (K_f, D_f, l_f), sample (K_s, D_s, l_s), black layer (K_c, D_c, l_c) and backing (K_b, D_b, l_b). Assuming that all the light is absorbed only by the black layer, the heat equations in the different media are given by:

$$\begin{aligned}
&\frac{\partial^2 T_f}{\partial z^2} = \frac{1}{D_f}\frac{\partial T_f}{\partial t} && if\ 0 \le z \le l_f \\
&\frac{\partial^2 T_c}{\partial z^2} = \frac{1}{D_c}\frac{\partial T_c}{\partial t} - A_c e^{\alpha_c z}\left(1 + e^{j\omega t}\right) && if\ -l_c \le z \le 0 \\
&\frac{\partial^2 T_s}{\partial z^2} = \frac{1}{D_s}\frac{\partial T_s}{\partial t} && if\ -l_c - l_s \le z \le -l_s \\
&\frac{\partial^2 T_b}{\partial z^2} = \frac{1}{D_b}\frac{\partial T_b}{\partial t} && if\ -l_c - l_s - l_b \le z \le -l_c - l_s
\end{aligned} \tag{6}$$

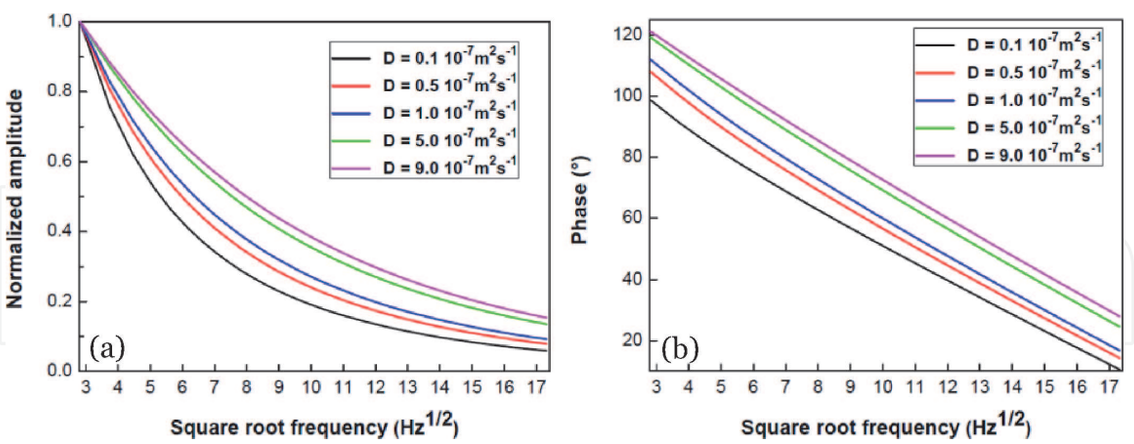

Figure 3.
Theoretical variation of the normalized amplitude (a) and phase (b) of the photothermal signal with the square root of modulation frequency for different values of thermal diffusivity.

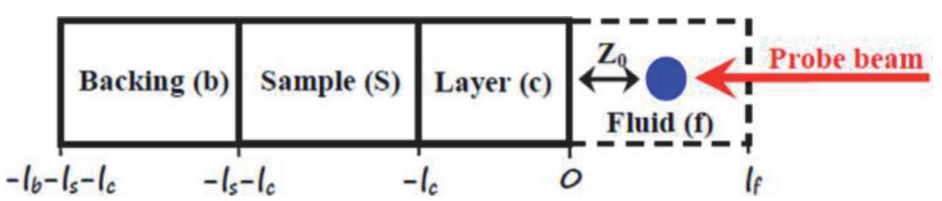

Figure 4.
Different medium.

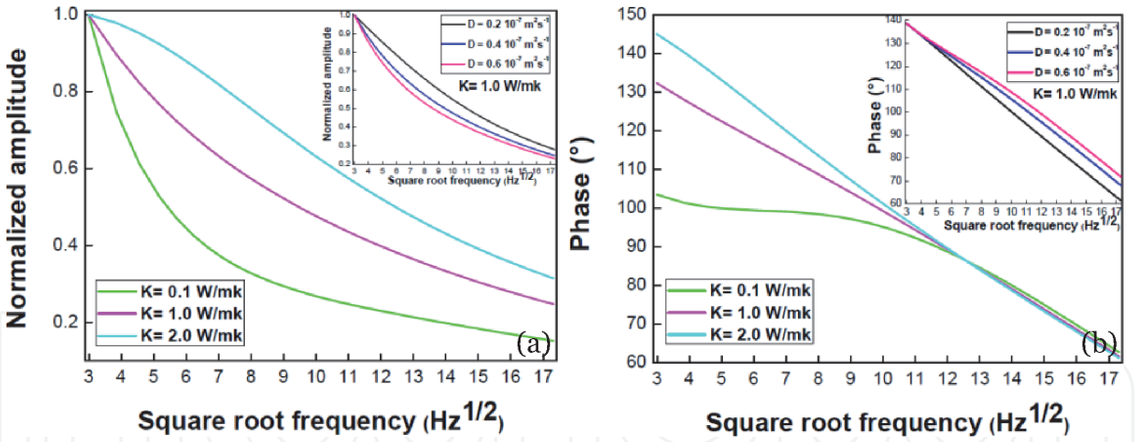

Figure 5.
Theoretical variation of the normalized amplitude (a) and phase (b) of the photothermal signal with the square root of modulation frequency for three values of thermal diffusivity and thermal conductivity.

where $A_c = \alpha_c I_0/2k_c$ are constant numbers and α_c is the optical absorption coefficient of the black layer.

By applying the continuity conditions of temperature and heat flow at the different interfaces allows us to determine the expression of the periodic temperature T_0 at the sample surface:

$$\begin{aligned} T_0 = E_c[&(1-b)e^{-\sigma_s l_s}[(1-r_c)(1-c)e^{\sigma_c l_c} + (1+r_c)(1+c)e^{-\sigma_c l_c} \\ &-2(1+c\,r_c)e^{-\alpha_c l_c}] - (1+b)e^{\sigma_s l_s}[(1-r_c)(1+c)e^{\sigma_c l_c} + (1+r_c)(1-c)e^{-\sigma_c l_c} \\ &-2(1-c\,r_c)e^{-\alpha_c l_c}]] \,/[(1+b)e^{\sigma_s l_s}\left[\left(1+\frac{g}{c}\right)(1+c)e^{\sigma_c l_c} + \left(1-\frac{g}{c}\right)(1-c)e^{-\sigma_c l_c}\right] \\ &-(1-b)e^{-\sigma_s l_s}\left[\left(1+\frac{g}{c}\right)(1-c)e^{\sigma_c l_c} + \left(1-\frac{g}{c}\right)(1+c)e^{-\sigma_c l_c}\right]] \end{aligned} \tag{7}$$

where $E_c = A_c/(\alpha_c^2 - \sigma_c^2)$, $r_c = \alpha_c/\sigma_c$, $b = k_b\sigma_b/k_s\sigma_s$, $c = k_c\sigma_c/k_s\sigma_s$, and $g = k_f\sigma_f/k_s$.

3.2.2.2 Illustration of theoretical model

Figure 5 shows the variations of normalized amplitude and phase for three values of thermal conductivity with equal thermal diffusivity $D = 0.4\ 10^{-7}\ m^2\ s^{-1}$ and well-defined values of the properties of the ink layer [11]. In addition, **Figure 5** also shows the variations normalized amplitude and phase for different values of thermal diffusivity with $k = 1\ Wm^{-1}\ K^{-1}$.

We notice that the PTD signal is sensitive to both the conductivity and the thermal diffusivity of sample (substrate). Since the value of thermal diffusivity is determined in the previous case (sample without layer), the value of thermal conductivity can be determined with great precision.

4. Determination of the thermal diffusivity of the samples (without black layer)

In this section, we will study the thermal diffusivity of samples (MOC without and with *PVAc*) using the Photothermal Deflection technique PTD. Thermal diffusivity is measured by the coincidence between the experimental curves of photothermal signal to the corresponding theoretical ones.

4.1 Thermal diffusivity of Sorel cement without PVAc

Figure 6 presents the experimental curves of normalized amplitude (a) and phase (b) of the photothermal signal and the corresponding theoretical ones for three values of the thermal diffusivity 0.2, 0.4 and 5.0 m^2/s versus square root modulation frequency for the reference sample (MOC without PVAc). Furthermore, **Figure 6** also presents the experimental normalized amplitude and phase of the photothermal signal and the corresponding theoretical ones for three values of the thermal conductivity 0.01, 0.3 and 0.7 w/mk versus the square root modulation frequency for magnesium oxychloride cement.

As noted in the previous section, the PTD signal is insensitive to thermal conductivity. We can only determine the values of the thermal diffusivity of the magnesium oxychloride cement. The theoretical curve which coincides best with the experimental curve is obtained for 0.4 10^{-7} m^2 s^{-1}.

4.2 Thermal diffusivity of Sorel cement with PVAc

We will proceed the same way for the rest of the magnesium oxychloride cement samples to which PVAc has been added with different percentages using the same method. **Figure 7** shows the normalized amplitude and phase of experimental

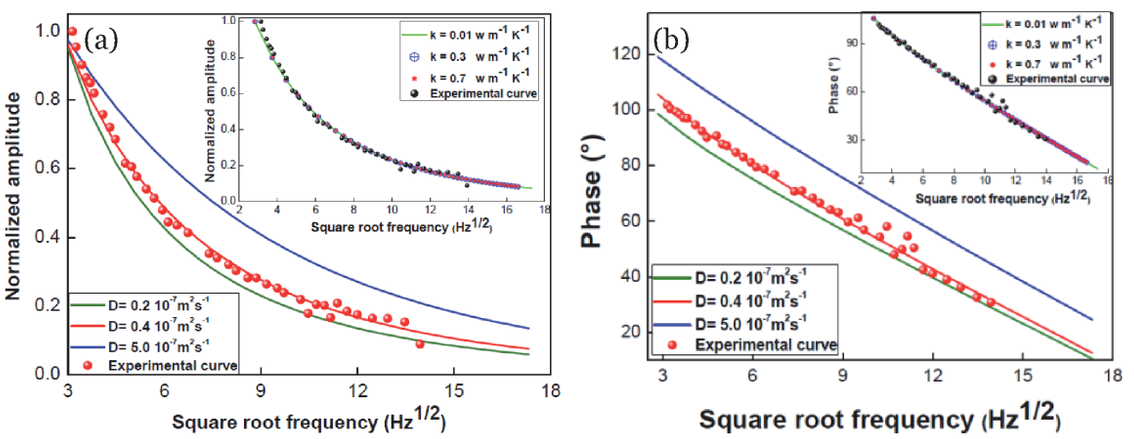

Figure 6.
Experimental and theoretical variation of the normalized amplitude (a) and phase (b) of the photothermal signal with the square root of modulation frequency for three values of thermal diffusivity and thermal conductivity.

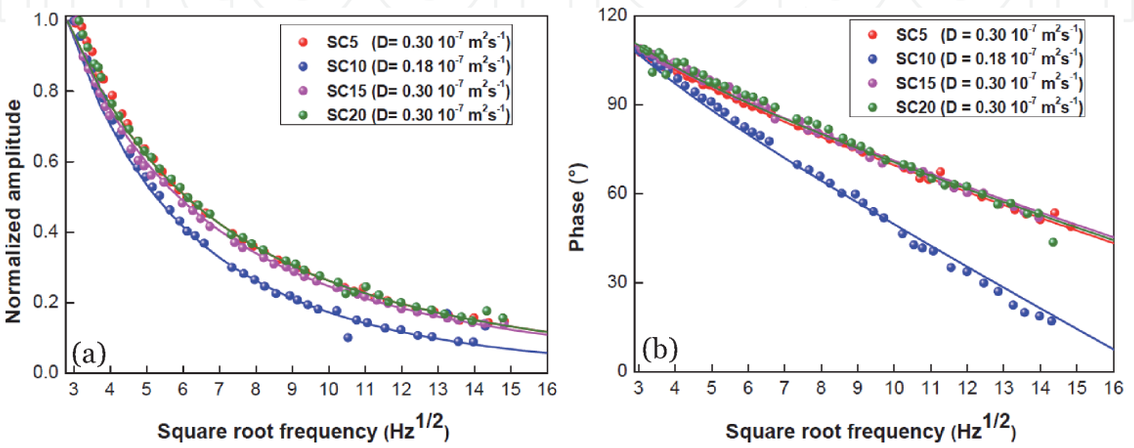

Figure 7.
The normalized amplitude (a) and phase (b) of experimental photothermal signal versus square root of modulation frequency of the magnesium oxychloride cement with PVAc fitted with theoretical curves (line).

photothermal signal versus square root of modulation frequency of the magnesium oxychloride cement with PVAc fitted with theoretical curves. The theoretical curves that best coincide with the experimental curves allow deducing the thermal diffusivity of the samples (**Figure 7**). The difference between theses curves is due to their different thermal diffusivity. We note that the addition of PVAc significantly influences on the diffusivity values. Indeed, the thermal diffusivity decreases with the percentage of PVAc and reaches their minimum values at 10% and begins to increase after this value. The reduction of thermal diffusivity of cement is due to the insulating effect of polyvinyl acetate particles. The thermal diffusivity of PVAc is measured by the same technique (PTD) [12].

5. Determination of the thermal conductivity of the samples (with black layer)

In order to determine the thermal conductivity value of the sample, we have deposed a thin ink layer of few microns thick at the sample surface which we have taken into account in our theoretical model. The ink layer absorbs the entire light beam and therefore considerably increases the amplitude of the photothermal signal and makes the signal sensitive to the thermal conductivity of the sample.

5.1 Thermal conductivity of Sorel cement without PVAc

Indeed, these curves represent the experimental and theoretical variation of normalized amplitude and phase of the photothermal signal versus the square root of the modulation frequency (**Figure 8**). The best adjustment is obtained for a thermal conductivity equal to 0.9 $Wm^{-1}K^{-1}$. This suggests that the thermal conductivity (0.9 $Wm^{-1}K^{-1}$) and thermal diffusivity (0.4×10^{-7} m^2 /s) values are reasonably accurate.

5.2 Thermal conductivity of Sorel cement with PVAc

The curves on **Figure 9** show the experimental and theoretical variation of the normalized amplitude (a) and phase (b) of the photothermal signal with the square root of modulation frequency. The best adjustment of experimental and theoretical curve leads to the determination of thermal conductivity value with precision. We notice that magnesium oxychloride cement (without PVAc) present the greatest

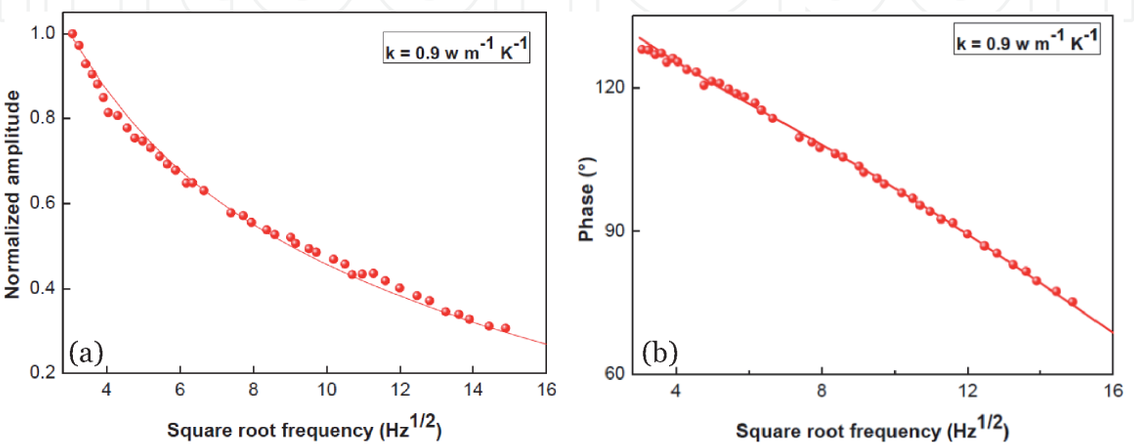

Figure 8.
Normalized amplitude (a) and phase (b) of experimental Photothermal signal versus square root modulation frequency of PVAc fitted with theoretical curves (line).

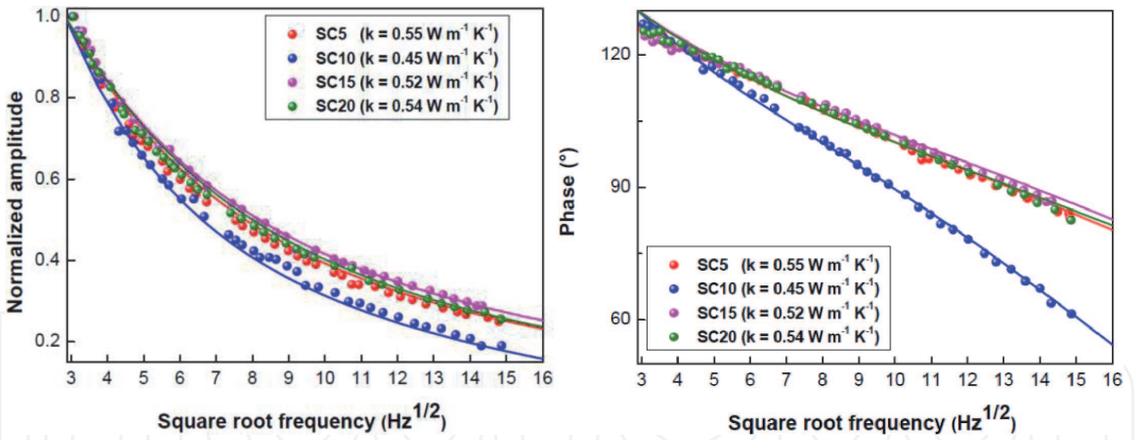

Figure 9.
Experimental and theoretical variation of the normalized amplitude (a) and phase (b) of the photothermal signal with the square root of modulation frequency.

values of thermal conductivity. The samples of magnesium oxychloride cement with different percentages present a minimum of thermal conductivity at 10% addition with a slight increase to 15 and 20% of PVAc. Indeed, the insulating effect and the amorphous structure of PVAc particles [11–12] are responsible for the reduction of thermal conductivity. We conclude that the incorporation of PVAc improves the thermal properties of the MOC. Values of thermal conductivity and thermal diffusivity decreased from 0.9 to 0.45 w/mk, and 0.4×10^{-7} to 0.18×10^{-7} m^2/s, respectively. Moreover, an optimum of 10% is obtained, which corresponds to a reduction of approximately 50% in thermal conductivity and 55% in thermal diffusivity which can be explained by the appearance of the smallest pore-size in the cement matrix [12].

6. Compressive strength

In order to study the effect of the incorporation of polymers on the mechanical properties, compressive strength measurements made on samples air-cured for 28 days. The results of compressive strength are shown in **Table 1**.

The incorporation of PVAc losses the mechanical strength and it presents a variation from 64.88 to 23.07 MPa corresponds to a reduction approximately of 64%. Furthermore, the reduction in compressive strength of the thermal optimum is approximately 55%. However, it maintains good mechanical strength. Indeed, we improve the thermal properties of magnesium oxychloride cement while keeping a good resistance. The phase 5 ($5\ Mg(OH)_2.MgCl_2.8H_2O$) is the source for strength and hardening of Sorel cement. At the atomic scale, phase 5 formation can be explained by the adsorption of the atoms Mg^{2+}, OH^- and Cl^- when mixing MgO and $MgCl_2.6H_2O$ on the surface of MgO. **Figure 10** shows the microstructures of both magnesium

Samples	Compressive strength (MPa)
SC0	64.88
SC5	41.33
SC10	29.05
SC15	26.40
SC20	23.07

Table 1.
Compressive strength of Sorel cement for different percentage of PVAc.

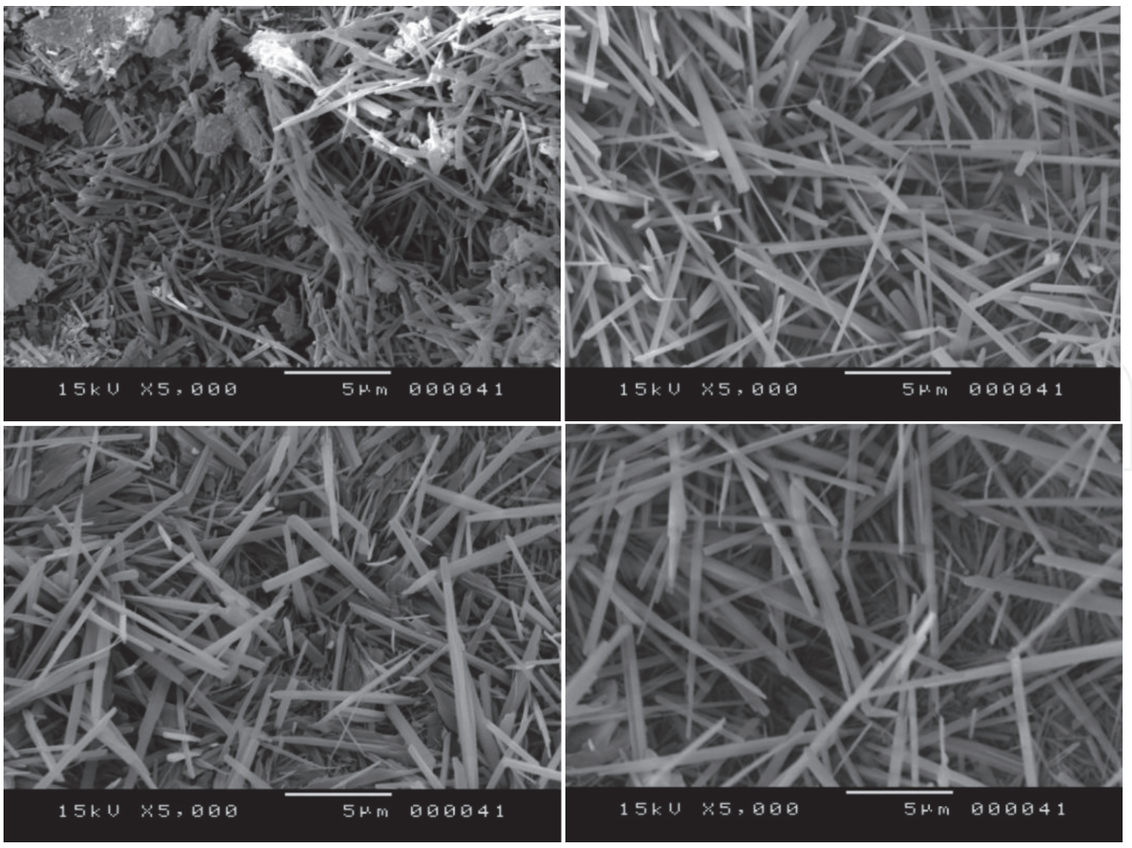

Figure 10.
Microstructure of SC5, SC10, SC15 and SC20.

oxychloride cement without and with PVAc (5 μm). We see in these images the needle shaped crystals. These needles shaped crystals is the P5 ($5Mg(OH)_2.MgCl_2.8H_2O$). We note that the incorporation of PVAc does not affect for the development of P5.

7. Conclusion

The objective of this work is to study the thermal properties of Sorel cement, which is a building material with promising performance. In order to determine the thermal properties of the cement, the photothermal deflection technique is used. The insulation properties of the SC were enhanced with the incorporation of PVAc. The thermal conductivities and thermal diffusivity of SC with PVAc are in a range of 0.45–0.9 W/m K and 0.4 10^{-7}–0.18 10^{-7} m^2/s, respectively. A thermal optimum is obtained for 10% of PVAc so that a reduction of 50% of the thermal conductivity and 55% of the thermal diffusivity is obtained. Furthermore, the compressive strength of SC is notably influenced by the incorporation of PVAc and increases with decreasing PVAc percentages, the value of compressive strength vary from 64.88 to 23.07 MPa and achieves a reduction of up to 64% for 20% of PVAc. However, the thermal optimum reaches 55% reduction in compressive strength (29.05 MPa) but retains good mechanical strength.

Acknowledgements

This chapter was supported by a grant from Ministry of Higher Scientific Research of Tunisia. The authors would like to thank the technical team of the

physics mathematics quantum modeling and mechanical design laboratory in Preparatory Institute for Engineering Studies of Nabeul and the National Research Centre of Materials Sciences in Borj Cedria Technological Park.

Author details

Rim Zgueb[1*], Amal Brichni[2] and Noureddine Yacoubi[1]

1 Physics Mathematics Quantum Modeling and Mechanical Design, Preparatory Institute for Engineering Studies of Nabeul, Nabeul, Tunisia

2 Useful Material Valorization Laboratory, National Center for Research in Materials Sciences, Technopole Borj Cedria, Soliman, Tunisia

*Address all correspondence to: rim.zgueb@fsb.u-carthage.tn

References

[1] Sorel. Improved composition to be used as a cement and as a plastic material for molding various articles. U.S. Patent; 1866. pp. 53-92

[2] Saad SM, Nasser S, Aboterika HA. Removal of synthetic reactive dyes from textile wastewater by Sorel's cement. Journal of Hazardous Materials. 2009; **162**:994-999

[3] Maravelaki KP, Moraitou G. Sorel's cement mortars decay susceptibility and effect on pentelic marble. Cement and Concrete Research. 1999;**29**:1929-1935

[4] Ji YS. Step by step building of a model for the berkovich indentation cycle. Materials Letters. 2002;**56**:353-356

[5] Cole WF, Demediuk H. X-ray thermal and dehydration studies on magnesium oxychloride. Division of Building Research. 1954;**5**:234-251

[6] Alegret S, Blanco M, Subirats R. Potentiometric study of the reactivity of calcined magnesium for use in magnesium oxychloride cements. Journal of the American Ceramic Society. 1984;**67**:579-582

[7] Beaudoin JJ, Ramachandran VS. Strengh development in magnesium. Cement and Concrete Research. 1975;**5**: 617-630

[8] Yu H. Magnesium Oxychloride Cement and Its Application. 1st ed. Beijing: China Building Materials Industry Press; 1993

[9] Zongjini L, Chau CK. Influence of molar ratios on properties of magnesium oxychloride cement. Cement and Concrete Research. 2007;**37**:866-870

[10] Fernelius NC. Extension of the Rosencwaig-Gersho photoacoustic spectroscopy theory to include effects of a sample coating: Applied Optics. 1980: 23-16

[11] Zgueb R. Contribution to the Study of the Thermal Properties of Sorel Cement by the Photothermal Deflection Technique. Tunisia: University of Carthage; 2019

[12] Zgueb R, Brichni A, Yacoubi N. Improvement of the thermal properties of Sorel cements by polyvinyl acetate: Consequences on physical and mechanical properties. Energy and Buildings. 2018;**169**:1-8